Energy Advances

ROYAL SOCIETY OF CHEMISTRY

PAPER

View Article Online
View Journal | View Issue

Cite this: *Energy Adv.*, 2023, 2, 1030

A chlorinated polythiophene-based polymer as a dopant-free hole transport material in perovskite solar cells†

Kakaraparthi Kranthiraja, [a] Ryosuke Nishikubo [ab] and Akinori Saeki *[ab]

Received 14th March 2023,
Accepted 24th May 2023

DOI: 10.1039/d3ya00113j

rsc.li/energy-advances

Despite the remarkable strides made in perovskite solar cell (PSC) research, the incorporation of doped hole transport materials (HTMs) presents a commercialization bottleneck. This study presents a chlorine-substituted polythiophene-based, dioxobenzodithiophene-containing conjugated polymer (P2T-Cl) as a promising dopant-free HTM. The highest occupied molecular orbital of P2T-Cl aligns well with PSCs, and flash-photolysis time-resolved microwave conductivity (TRMC) measurements reveal a high hole transfer yield of 0.99 for P2T-Cl compared to the non-chlorinated analogue of P2T (0.97) and non-doped polytriarylamine (PTAA) (0.79). Consequently, P2T-Cl exhibits a higher power conversion efficiency (PCE) without dopants (15.40%) compared to P2T (15.18%) and the standard polymer HTM PTAA (12.74%). This work presents a compelling example of a dopant-free polymer HTM with a simple structure for PSCs.

Introduction

Perovskite solar cells (PSCs) have been brought into sharp focus in the photovoltaic field owing to their excellent performance in recent years.[1–5] Recently, the power conversion efficiency (PCE) has reached 25.7%, which is based on the outstanding inherent properties of perovskite materials as well as the progressive optimization of each functional layer, especially the active layer and charge transporting material.[6–10] Apart from their high device performance, long-term stability is a major challenge in PSC research, which is a bottleneck for their practical use.[11–14] The most widely used perovskite absorbers ($APbI_3$, A = MA, FA, or Cs; MA: methylammonium cation, FA: formamidinium cation) are prone to readily decompose into their precursors upon exposure to moisture, high temperature, and external stress.[15–18] Henceforth, many stable perovskite absorbers were successfully amended in PSCs to improve their long-term stability. Besides the external dopants such as lithium bis-(trifluoromethanesulfonyl)imide (Li-TFSI) associated with hole transport materials (HTMs) of spiro-OMeTAD (2,2′,7,7′-tetrakis(*N*,*N*-di-*p*-methoxyphenylamine)-9,9′-spirobifluorene) and polytriarylamine (PTAA) are hygroscopic.[19–22] This deliquescent behaviour of hygroscopic dopants tends to trap moisture and degrade the perovskite material and causes serious damage to the overall device performance and longevity.[23–25] Thus sole engineering of perovskites might not be sufficient to improve the overall stability of PSCs. So far, this critical issue has been well-addressed by designing several types of dopant-free molecular HTMs[26–30] or polymeric HTMs.[31–45] However, the molecular HTMs still suffer from issues like low charge transport, poor surface morphology, and require large quantity of materials to make a film.[46] For instance, the concentration of a standard molecular spiro-OMeTAD is 70–90 mg mL^{-1} for a lab scale experiment (Fig. S1a (ESI†)). In contrast, dopant-free polymer HTMs have intrinsic merits like high charge transport, excellence of film formation, and requirement of a small quantity for making a smooth film successfully address many issues concerning ideal HTMs. Incidentally, a lower concentration (5–10 mg mL^{-1}) of polymer is enough to achieve a high-quality film (Fig. S1b (ESI†)) for a lab scale experiment. However, most of the polymer HTM synthesis involves expensive raw materials, and complex synthesis with poor yields, which is also a hurdle for commercialization.[29,30] In this regard, polymer HTMs with limited synthetic steps are intriguing to study and realize their practical use in PSCs.[47] Although polythiophene-based polymers like poly(3-hexylthiophene) (P3HT, Fig. S1c (ESI†)) became a successful candidate (readily available from various commercial vendors) for various organic electronics, the

[a] *Department of Applied Chemistry, Graduate School of Engineering, Osaka University, 2-1 Yamadaoka, Suita, Osaka 565-0871, Japan. E-mail: saeki@chem.eng.osaka-u.ac.jp*
[b] *Innovative Catalysis Science Division, Institute for Open and Transdisciplinary Research Initiatives (ICS-OTRI), Osaka University, 1-1 Yamadaoka, Suita, Osaka 565-0871, Japan*

† Electronic supplementary information (ESI) available: Synthesis, experimental, optical spectra, TRMC results, and device results. See DOI: https://doi.org/10.1039/d3ya00113j

limited tunability of its optoelectronic properties limits its applicability to various applications.[48] Thus exploration of alternative conjugated polymers with scalable features is necessary in the field of organic/perovskite photovoltaics. Incidentally, chlorine-substituted polymers are interesting owing to their inherent optoelectronic properties with minimal synthesis and low-cost reagents when they are compared to the high-performance fluorine substituted polymers. This feature seems suitable for organic functional materials that are practically viable for a large-scale production. Notably, such chlorinated photoactive materials with limited synthetic steps successfully demonstrated comparable optoelectronic properties and performances to fluorine based photoactive materials.[49–52]

On the other hand, imperfections in perovskites have a strong impact on the PCE and stability of PSCs, especially due to the charge trap. These traps often show a detrimental effect on the overall PSC performance. Hence it is imperative to establish techniques that reduce the trap density of perovskites. It has been manifested that Lewis bases can donate a pair of nonbonding electrons to passivate undercoordinated Pb^{2+} or Pb clusters, forming a Lewis adduct. The Lewis adducts can reduce the nonradiative charge recombination and improve the lifetime to enhance the perovskite device performance and stability. Pyridine and thiophene were the first ever reported materials as Lewis bases. Later, molecules with nitrogen, sulfur, oxygen, and phosphorus functionalities would work as Lewis bases to passivate the defects in perovskite materials.[53] In this connection, both P2T and P2T-Cl with multiple sulfur atoms on their backbone would passivate the perovskite surface. Thus, we firmly believe that exploration of new chlorine substituted polymer HTMs would bring significant advances in the PSC performance and their long-term stability.

In this work, we report a new chlorinated polythiophene polymer HTM of poly(1-(3″-chloro-3-(2-ethylhexyl)-5″-[2,2′:5′,2″-terthiophen]-5-yl)-*alt*-5,7-bis(2-ethylhexyl)-3-(4-(2-ethylhexyl)-5-fluorothiophen-2-yl)-4*H*,8*H*-benzo[1,2-*c*:4,5-*c*′]dithiophene-4,8-dione) (P2T-Cl) for PSCs. It shows encouraging intrinsic merits like the suitable highest occupied molecular orbital (HOMO) with a perovskite valence band maximum, high hole transfer yield (0.99), and high hydrophobic nature. The optimized dopant-free P2T-Cl-based PSCs showed a maximum PCE of 15.40%, which is higher than those of the non-chlorinated P2T (15.18%) and standard PTAA (12.74%). In addition, the P2T-Cl was successfully incorporated into the lead-free solar cells (SbSI:Sb_2S_3 as a photo absorber), and it showed a decent PCE of 1.68% which is higher than those of the undoped PTAA (PCE: 0.37%) based PSCs.

Results and discussion

The molecular structure of P2T-Cl is shown in Fig. 1(a), and the polymer synthesis details are shown in the ESI† (Scheme S1 (ESI†); ^{1}H NMR of P2T-Cl in Fig. S2 (ESI†)). The number-averaged molecular weight (M_n) and polydispersity index (PDI) of the P2T-Cl were 16.4 kg mol^{-1} and 1.5, respectively.

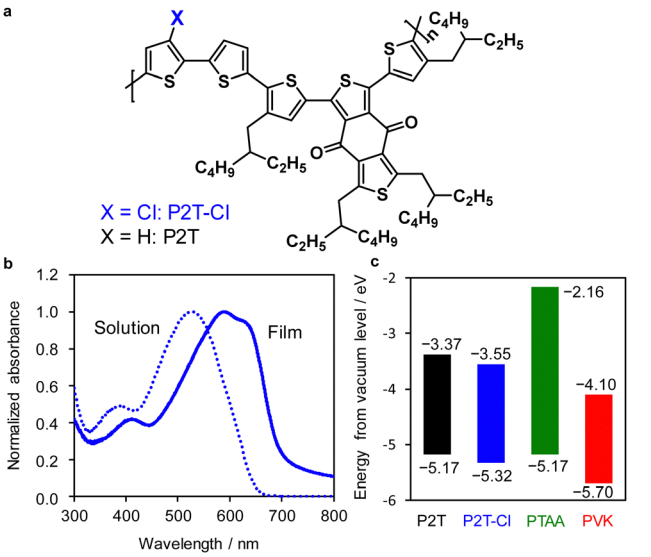

Fig. 1 (a) Chemical structure of P2T-Cl. (b) UV-vis spectra of P2T-Cl in CB (dotted line) and its film (solid line). (c) Energy level diagram P2T,[54] P2T-Cl, PTAA[53] and perovskite (PVK).[55] HOMO and LUMO levels were obtained from photoelectron yield spectroscopy (Fig. S3 (ESI†)) and HOMO + E_g, respectively.

We repeated the polymer synthesis three more times, where the resulting polymer PDIs (1.4–1.6) were maintained well aligned with the first polymer batch. As presented in Fig. 1(b), the photoabsorption spectra of P2T-Cl are ranging from 300–650 nm in solution and 300–750 nm in the film state. Energy levels of P2T, P2T-Cl, and PTAA are shown in Fig. 1(c). Density functional theory (DFT) (B3LYP/6-31G*) calculations were performed for P2T-Cl to understand the electronic properties (Fig. S4 and S5 (ESI†)). The HOMO and the lowest unoccupied molecular orbital (LUMO) levels of P2T-Cl were calculated to be −5.19 eV and −2.31 eV, respectively (Fig. S4 (ESI†)). The front and side view images with dihedral angles are shown in Fig. S5 (ESI†), where the relatively planar backbone and moderate dipole moment (1.23 D) value of P2T-Cl is relevant to a good packing behaviour of the polymer in the film state.

To provide an insight into the hole transfer process, flash-photolysis time-resolved microwave conductivity (TRMC) evaluations were performed for the quartz/mesoporous (mp)-TiO_2/perovskite with/without P2T, P2T-Cl and PTAA (Fig. S6 (ESI†)). The transient hole transfer yield (η_{HT}) was evaluated from the comparison of mp-TiO_2/perovskite and mp-TiO_2/perovskite/HTM films for each polymer (Fig. 2).[54] The highest hole transfer yield in the saturated region (*ca.* 8 μs) (η_{sat}) of 0.99 was found for P2T-Cl, followed by P2T (0.97) and PTAA (0.79). The delayed hole transfer rates (k) are P2T: 9.5 × 10^5 s^{-1}, P2T-Cl: 1.2 × 10^6 s^{-1}, PTAA: 9.8 × 10^4 s^{-1}, respectively (Fig. S7 (ESI†)),[54,55] which indicates the superior hole transfer of P2T-Cl to the others.

The impact of P2T-Cl as a HTM on the photovoltaic outputs was examined by fabricating dopant-free PSCs in a regular device structure (FTO/compact-TiO_2/mp-TiO_2/perovskite/HTM/Au). Herein, we used $(FAPbI_3)_{0.87}$ $(MAPbBr_3)_{0.13}$ as a perovskite absorber considering its superior features over $MAPbI_3$.[56,57]

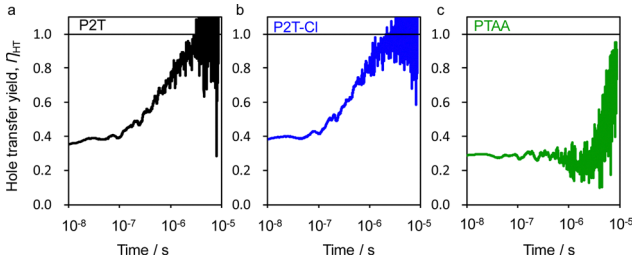

Fig. 2 Semilogarithmic plot of time-dependent hole transfer yields from perovskites to non-doped polymer HTM of (a) P2T, (b) P2T-Cl, and (c) PTAA evaluated by flash-photolysis TRMC (λ_{ex} = 500 nm, photon density is 2.6 × 10^{10} photons cm^{-2} $pulse^{-1}$).

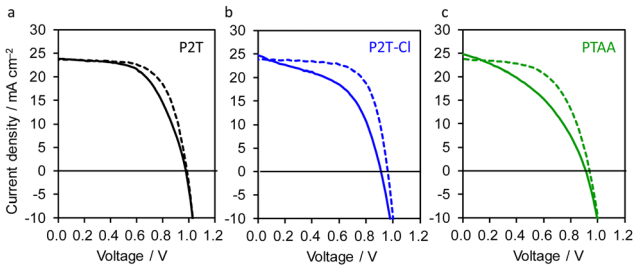

Fig. 3 Optimized *J*–*V* dopant-free (a) P2T (b) P2T-Cl and (c) PTAA based PSCs. The solid and dotted lines are forward and reverse scans, respectively.

The optimized current density (*J*) and voltage (*V*) curves for the P2T, P2T-Cl and PTAA based PSCs are shown in Fig. 3, while their external quantum efficiency (EQE) spectra are shown in Fig. S8 (ESI†). Interestingly, P2T-Cl delivered the maximum PCE of 15.40%, which was slightly higher than P2T (15.18%) but much more improved than PTAA (12.74%) (Table 1). Notably, we found a good correlation between the maximum PCE, and hole transfer yield obtained from TRMC (HTM/PCE/η_{sat}: P2T-Cl/15.40%/0.99, P2T/15.18%/0.97 and PTAA/12.74%/0.79). The enhanced PCE of P2T-Cl based PSCs is mainly due to the improved short-circuit current density (J_{SC}) and fill factor (FF) over P2T and PTAA. The low PCE of P2T and PTAA could be due to their poor charge transport properties owing to their disordered orientation and low crystallinity. Although the P2T-Cl and P2T-based PSCs did not show outstanding PCE values, they successfully surpassed the PCE of PTAA (undoped) and showed the advantage of developing simple structured polythiophene-based HTMs. In addition, we extended P2T-Cl into the lead-free, solution-processed solar cells (SbSI:Sb_2S_3 composite as an absorber) as an HTM, demonstrating the maximum PCE of 1.68% (Fig. S9a (ESI†)) with J_{SC} = 7.41 mA cm^{-2}, open-circuit voltage (V_{OC}) = 0.45 V, and FF = 0.49, which is superior to that of the non-doped PTAA (PCE: 0.37%; Fig. S9b (ESI†)). Altogether, it is evident that the simple structure polythiophene-based polymers (P2T and P2T-Cl) found to be interesting candidates for being alternate polymer HTMs to the expensive PTAA. The price comparison for P2T-Cl, PTAA, and P3HT are given in Table S1 (ESI†).

Table 1 Optimized photovoltaic performances of the non-doped PTAA, P2T and PT2T-Cl based PSCs

HTM	J_{sc}/mA cm^{-2}	V_{OC}/V	FF/%	PCE[a]/%	HI[b]
P2T	23.62	0.98	65	15.18 (13.50)	0.10
P2T-Cl	23.81	0.96	67	15.40 (14.77)	0.26
PTAA	23.76	0.94	56	12.74 (11.36)	0.27

[a] Values in the parentheses are average values of four to six individual devices. [b] Hysteresis index = $(PCE_{reverse} - PCE_{forward})/PCE_{reverse}$.

In addition to the photovoltaic characters, we measured the surface texture of pristine by atomic force microscopy (AFM) as shown in Fig. 4(a)–(c). P2T, P2T-Cl and PTAA showed a smooth morphology with root-mean-square roughness values of 2.13, 1.57, and 0.33 nm, respectively. This partly reveals that these polymers exhibit sufficient coverage of perovskite without aggregation. Since charge transport properties of the polymers are highly reliant on their packing and orientation, we then analysed the polymer films by two-dimensional grazing incidence X-ray diffraction (2D-GIXRD). The 2D-GIXRD images of P2T, P2T-Cl and PTAA are shown in Fig. 4(d)–(f). The in-plane and out-of-plane profiles are shown in Fig. S10 (ESI†). Furthermore, surface morphology of P2T, P2T-Cl and PTAA on the perovskite surface are shown in Fig. S11 (ESI†). P2T-Cl showed a slightly reduced surface roughness compared to P2T and PTAA.

Notably, P2T-Cl showed an intense π–π stack diffraction over P2T and PTAA. The intensity ratio of the in-plane (I_{IP}) to the out-of-plane (I_{OOP}) direction (I_{IP}/I_{OOP}) is an indicator of polymer orientation (I_{IP}/I_{OOP} ∼ 0: edge-on; I_{IP}/I_{OOP} ∼ 1: random; I_{IP}/I_{OOP} > 1: face-on). P2T-Cl indicated a face-on

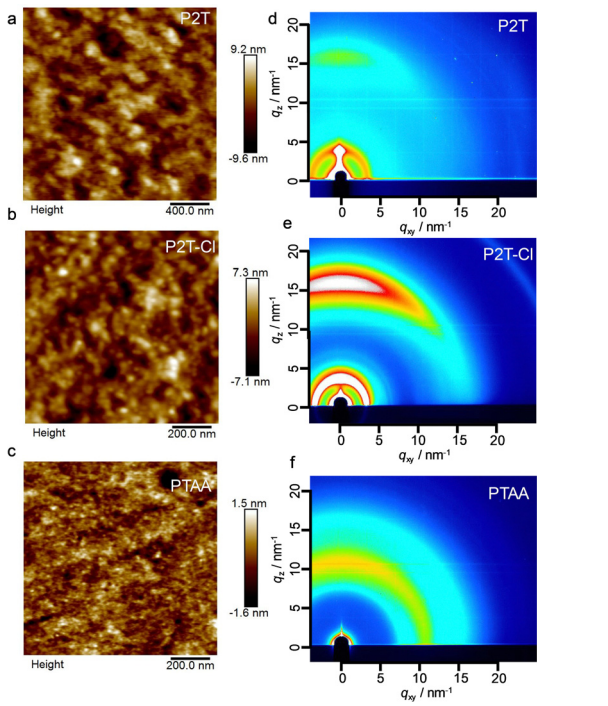

Fig. 4 (a)–(c) AFM images and (d)–(f) 2D-GIXRD images of P2T, P2T-Cl, and PTAA polymer films.

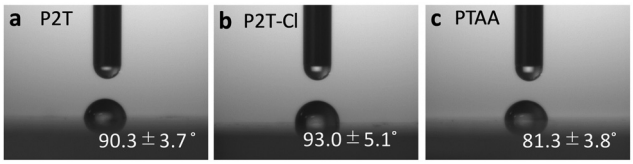

Fig. 5 (a)–(c) Water contact angles of P2T, P2T-Cl and PTAA.

orientation (I_{IP}/I_{OOP} = 1.02), whereas P2T is random (I_{IP}/I_{OOP} = 0.73) and PTAA is completely amorphous (Table S2 (ESI†)). Chlorine substitution in the polymer backbone would improve the enhanced intermolecular interactions, and pre-aggregation is responsible for the preferential face-on orientation of P2T-Cl compared to P2T.[51,58,59] The improved π–π stacking of P2T-Cl over P2T and PTAA could be a possible reason for the better alignment of polymer chains on the perovskite surface eventually resulting in efficient charge transport at the interface.

We then measured the water contact angle (WCA) for the three polymers (P2T, P2T-Cl and PTAA) and found the values to be 90.3 ± 3.7°, 93.0 ± 5.1° and 81.3 ± 3.8°, respectively (Fig. 5(a)–(c)). P2T-Cl showed a slightly higher WCA over the other two polymers, which could be attributed to the chlorine atom present in the polymer backbone. The higher hydrophobicity of the polymer HTM has been proven to be a plausible reason for the improved stability of PSCs.[32–36] Thus, it is presumed that the P2T and P2T-Cl based PSCs would show higher water repelling behaviour compared to PTAA. This enhanced hydrophobicity would certainly help in improving the overall stability of PSCs by protecting the photo absorber from moisture.[32–36]

The long-term stability of PSCs is a critical point to be addressed as it is a limiting parameter in commercialization. Thus, we performed the long-term stability test for P2T, P2T-Cl and PTAA based PSCs stability at 30 °C and relative humidity of 60% (dark, in an environment chamber). The long-term stability of P2T, P2T-Cl and PTAA based PSCs are shown in Fig. 6. P2T-Cl showed a relatively improved stability over the P2T and PTAA based PSCs. This could be attributed to the better hydrophobic nature of P2T-Cl and better coverage on the perovskite surface compared to the P2T and PTAA.

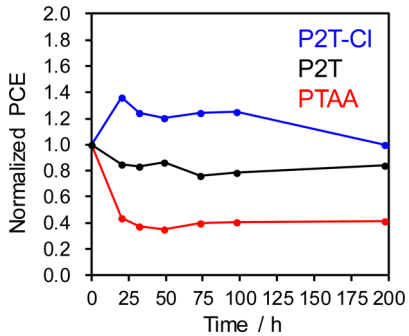

Fig. 6 Long-term stability of P2T, P2T-Cl and PTAA based PSCs. The PSCs were stored in an environmental test chamber at 30 °C and relative humidity of 60% in darkness.

Conclusions

In summary, this study reports the successful synthesis of a dopant-free HTM, chlorine-substituted polythiophene polymer (P2T-Cl), with a decent PCE of 15.40%. Intriguingly, P2T-Cl demonstrated a superior PCE compared to the non-doped PSCs based on P2T and PTAA. The high PCE of P2T-Cl can be attributed to its aligned HOMO with the perovskite, well-oriented film with intense π–π stacking, and high hole transfer yield (0.99). Additionally, the smooth surface morphology and high hydrophobicity contribute to the improved PCE. Notably, P2T-Cl is not only compatible with lead-based PSCs but can also be utilized in lead-free solar cells (SbSI:Sb_2S_3). This work provides a significant example of a simple polythiophene-based polymer HTM that outperforms PTAA for both lead and lead-free PSCs.

Conflicts of interest

The authors declare no competing financial interests.

Acknowledgements

This work was supported by the Japan Society for the Promotion of Science (JSPS) with the KAKENHI Grant-in-Aid for Scientific Research (A) (grant no. JP16H02285 and JP20H00398), and Grant-in-Aid for Transformative Research Areas, ''Dynamic Exciton'' (grant no. JP 20H05836), and the Japan Science and Technology Agency (JST) for Core Research for Evolutional Science and Technology (CREST) (grant no. JPMJCR2107) and MIRAI Program (grant no. JPMJMI22E2) and the New Energy and Industrial Technology Development Organization (NEDO), Green Innovation Project (JP21578854). K. K. acknowledges the JSPS Research Fellowship for Young Scientists (grant no. JP18F180350). The authors thank Dr Tomoyuki Koganezawa at JASRI for his support during the 2D-GIXRD experiments at SPring-8 (Proposals 2019A1765, 2020A1742, and 2020A1875).

References

1 A. Kojima, K. Teshima, Y. Shirai and T. Miyasaka, *J. Am. Chem. Soc.*, 2009, **131**, 6050–6051.
2 J. Y. Kim, J.-W. Lee, H. S. Jung, H. Shin and N.-G. Park, *Chem. Rev.*, 2020, **120**, 7867–7918.
3 L. Mao, C. C. Stoumpos and M. G. Kanatzidis, *J. Am. Chem. Soc.*, 2019, **141**, 1171–1190.
4 J. S. Manser, J. A. Christians and P. V. Kamat, *Chem. Rev.*, 2016, **116**, 12956–13008.
5 W. Zhang, G. E. Eperon and H. J. Snaith, *Nat. Energy*, 2016, **1**, 16048.
6 Z. Yu and L. Sun, *Adv. Energy Mater.*, 2015, **5**, 1500213.
7 S. Ameen, M. A. Rub, S. A. Kosa, K. A. Alamry, M. S. Akhtar, H.-S. Shin, H.-K. Seo, A. M. Asiri and M. K. Nazeeruddin, *ChemSusChem*, 2016, **9**, 10–27.

8 S. F. Volker, S. Collavini and J. L. Delgado, *ChemSusChem*, 2015, **8**, 3012–3028.
9 M. A. Green, E. D. Dunlop, J. Hohl-Ebinger, M. Yoshita, N. Kopidakis and A. W. Y. Ho-Baillie, *Prog. Photovoltaics*, 2020, **28**, 3–15.
10 R. Lin, K. Xiao, Z. Qin, Q. Han, C. Zhang, M. Wei, M. I. Saidaminov, Y. Gao, J. Xu, M. Xiao, A. Li, J. Zhu, E. H. Sargent and H. Tan, *Nat. Energy*, 2019, **4**, 864–873.
11 L. Duan and A. Uddin, *Mater. Chem. Front.*, 2022, **6**, 400–417.
12 C. C. Boyd, R. Cheacharoen, T. Leijtens and M. D. McGehee, *Chem. Rev.*, 2019, **119**, 3418–3451.
13 L. Meng, J. You and Y. Yang, *Nat. Commun.*, 2018, **9**, 5265.
14 Z. Qiu, N. Li, Z. Huang, Q. Chen and H. Zhou, *Small Methods*, 2020, **4**, 1900877.
15 C. Zheng and O. Rubel, *J. Phys. Chem. C*, 2019, **123**, 19385–19394.
16 E. Smecca, Y. Numata, I. Deretzis, G. Pellegrino, S. Boninelli, T. Miyasaka, A. L. Magna and A. Alberti, *Phys. Chem. Chem. Phys.*, 2016, **18**, 13413–13422.
17 Z. Yao, W. Zhao and S. Liu, *J. Mater. Chem. A*, 2021, **9**, 11124–11144.
18 S. Zhang and G. Han, *Prog. Energy*, 2020, **2**, 022002.
19 K. Rakstys, C. Igci and M. K. Nazeeruddin, *Chem. Sci.*, 2019, **10**, 6748–6769.
20 N. H. Tiep, Z. Ku and H. J. Fan, *Adv. Energy Mater.*, 2016, **6**, 1501420.
21 S. Wang, Z. Huang, X. Wang, L. Li, M. Günther, S. Valenzuela, P. Parikh, A. Cabreros, W. Xiong and Y. S. Meng, *J. Am. Chem. Soc.*, 2018, **140**, 16720–16730.
22 Y. Shi, X. Wang, H. Zhang, B. Li, H. Lu, T. Ma and C. Hao, *J. Mater. Chem. A*, 2015, **3**, 22191–22198.
23 Q. Wang, N. Phung, D. D. Girolamo, P. Vivo and A. Abate, *Energy Environ. Sci.*, 2019, **12**, 865–886.
24 B. Conings, J. Drijkoningen, N. Gauquelin, A. Babayigit, J. D'Haen, L. D'Olieslaeger, A. Ethirajan, J. Verbeeck, J. Manca, E. Mosconi, F. De Angelis and H.-G. Boyen, *Adv. Energy Mater.*, 2015, **5**, 1500477.
25 J. H. Noh, S. H. Im, J. H. Heo, T. N. Mandal and S. I. Seok, *Nano Lett.*, 2013, **13**, 1764–1769.
26 P. Qin, S. Paek, M. I. Dar, N. Pellet, J. Ko, M. Grätzel and M. K. Nazeeruddin, *J. Am. Chem. Soc.*, 2014, **136**, 8516–8519.
27 Z. Li, Z. Zhu, C.-C. Chueh, S. B. Jo, J. Luo, S.-H. Jang and A. K.-Y. Jen, *J. Am. Chem. Soc.*, 2016, **138**, 11833–11839.
28 H. Nishimura, N. Ishida, A. Shimazaki, A. Wakamiya, A. Saeki, L. T. Scott and Y. Murata, *J. Am. Chem. Soc.*, 2015, **137**, 15656–15659.
29 A. Wakamiya, H. Nishimura, T. Fukushima, F. Suzuki, A. Saeki, S. Seki, I. Osaka, T. Sasamori, M. Murata, Y. Murata and H. Kaji, *Angew. Chem., Int. Ed.*, 2014, **53**, 5800–5804.
30 Y. Chen, X. Xu, N. Cai, S. Qian, R. Luo, Y. Huo and S. W. Tsang, *Adv. Energy Mater.*, 2019, **9**, 1901268.
31 T. Tong, T. Chao, K. Tina, L. Bobo, Z. Chaoyue, S. Ullrich, G. Deqing and H. Wei, *Macromolecules*, 2018, **51**, 7407–7416.
32 G.-W. Kim, G. Kang, J. Kim, G.-Y. Lee, H. I. Kim, L. Pyeon, J. Lee and T. Park, *Energy Environ. Sci.*, 2016, **9**, 2326–2333.
33 K. Kranthiraja, K. Gunasekar, H. Kim, A.-N. Cho, N.-G. Park, S. Kim, B. J. Kim, R. Nishikubo, A. Saeki, M. Song and S.-H. Jin, *Adv. Mater.*, 2017, **29**, 1700183.
34 Y. Kim, E. H. Jung, G. Kim, D. Kim, B. J. Kim and J. Seo, *Adv. Energy Mater.*, 2018, **30**, 1801668.
35 J. Lee, M. M. Byranvand, G. Kang, S. Y. Son, S. Song, G.-W. Kim and T. Park, *J. Am. Chem. Soc.*, 2017, **139**, 12175–12181.
36 H.-C. Liao, T. L. Dexter Tam, P. Guo, Y. Wu, E. F. Manley, W. Huang, N. Zhou, C. M. M. Soe, B. Wang, M. R. Wasielewski, L. X. Chen, M. G. Kanatzidis, A. Facchetti, R. P. H. Chang and T. J. Marks, *Adv. Energy Mater.*, 2016, **6**, 1600502.
37 M. M. Tavakoli, J. Zhao, R. Po, G. Bianchi, A. Cominetti, C. Carbonera and J. Kong, *Adv. Funct. Mater.*, 2019, 1905887.
38 T. Matsui, I. Petrikyte, T. Malinauskas, K. Domanski, M. Daskeviciene, M. Steponaitis, P. Gratia, W. Tress, J.-P. Correa-Baena, A. Abate, A. Hagfeldt, M. Gratzel, M. K. Nazeeruddin, V. Getautis and M. Saliba, *ChemSusChem*, 2016, **9**, 2567–2571.
39 G. W. Kim, J. Lee, G. Kang, T. Kim and T. Park, *Adv. Energy Mater.*, 2018, **8**, 1870018.
40 T. Tong, T. Chao, K. Tina, L. Bobo, Z. Chaoyue, S. Ullrich, G. Deqing and H. Wei, *Macromolecules*, 2018, **51**, 7407–7416.
41 Y. Kim, G. Kim, N. J. Jeon, C. Lim, J. Seo and B. J. Kim, *ACS Energy Lett.*, 2020, **5**, 3304–3313.
42 F. Zhang, Z. Yao, Y. Guo, Y. Li, J. Bergstrand, C. J. Brett, B. Cai, A. Hajian, Y. Guo, X. Yang, J. M. Gardner, J. Widengren, S. V. Roth, L. Kloo and L. Sun, *J. Am. Chem. Soc.*, 2019, **141**, 19700–19707.
43 X. Sun, X. Deng, Z. Li, B. Xiong, C. Zhong, Z. Zhu, Z. Li and A. K.-Y. Jen, *Adv. Sci.*, 2020, 1903331.
44 Z. Yao, F. Zhang, Y. Guo, H. Wu, L. He, Z. Liu, B. Cai, Y. Guo, C. J. Brett, Y. Li, C. V. Srambickal, X. Yang, G. Chen, J. Widengren, D. Liu, M. Gardner, L. Kloo and L. Sun, *J. Am. Chem. Soc.*, 2020, **142**, 17681–17692.
45 X. Sun, X. Yu and Z. Li, *ACS Appl. Energy Mater.*, 2020, **3**, 10282–10302.
46 L. Liang, N. Shibayama, H. Jiang, Z. Zhang, L. Meng, L. Zhang, C. Wang, N. Zhao, Y. Yu, S. Ito, J. Wu, J. Chen and P. Gao, *J. Mater. Chem. A*, 2022, **10**, 3409–3417.
47 D. D. Astridge, J. B. Hoffman, F. Zhang, S. Y. Park, K. Zhu and A. Sellinger, *ACS Appl. Polym. Mater.*, 2021, **3**, 5578–5587.
48 Y. Zhang, M. Elawad, Z. Yu, X. Jiang, J. Laia and L. Sun, *RSC Adv.*, 2016, **6**, 108888.
49 K. Kranthiraja, K. Murotani, F. Hamada and A. Saeki, *ACS Appl. Electron. Mater.*, 2022, **4**, 2086–2094.
50 P. Chao, N. Johner, X. Zhong, H. Meng and F. He, *J. Energy Chem.*, 2019, **39**, 208–216.
51 H. Yao, J. Wang, Y. Xu, S. Zhang and J. Hou, *Acc. Chem. Res.*, 2020, **53**, 822–832.
52 G. P. Kini, S. J. Jeon and D. K. Moon, *Adv. Mater.*, 2020, **32**, 1906175.
53 B. Chen, P. N. Rudd, S. Yang, Y. Yuan and J. Huang, *Chem. Soc. Rev.*, 2019, **48**, 3842–3867.

54 N. Ishida, A. Wakamiya and A. Saeki, *ACS Photonics*, 2016, **3**, 1678–1688.
55 K. Kranthiraja and A. Saeki, *ACS Appl. Polym. Mater.*, 2021, **3**, 2759–2767.
56 N. Minoi, F. Ishiwari, K. Murotani, R. Nishikubo, T. Fukushima and A. Saeki, *ACS Appl. Mater. Interfaces*, 2023, **15**, 6708–6715.
57 K. T. Cho, S. Paek, G. Grancini, C. Roldan-Carmona, P. Gao, Y. Lee and M. K. Nazeeruddin, *Energy Environ. Sci.*, 2017, **10**, 621–627.
58 Y.-Q. Zheng, Z. Wang, J.-H. Dou, S. D. Zhang, X.-Y. Luo, Z.-F. Yao, J.-Y. Wang and J. Pei, *Macromolecules*, 2015, **48**, 5570–5577.
59 J. S. Park, G. U. Kim, D. Lee, S. Lee, B. Ma, S. Cho and B. J. Kim, *Adv. Funct. Mater.*, 2020, **30**, 2005787.